Probing changes in frictional state due to normal stress perturbations using controlled-source ultrasonics

Srisharan Shreedharan[1]*, Jacques Rivière[2,1] and Chris Marone[1]

[1]Rock and Sediment Mechanics Laboratory, Pennsylvania State University, University Park PA 16802
[2]Engineering Science and Mechanics, Pennsylvania State University, University Park PA 16802
*Corresponding author: srisharan@psu.edu

Scan me to access the manuscript associated with this poster

T11F-0220

1. Introduction

Rate-state friction (RSF) represents the premier framework used in friction experiments and earthquake rupture models. An illustration of RSF is shown in Fig. 1. Fault behavior in response to velocity perturbations is well understood but the effect of normal stress is poorly quantified. Two contrasting sets of friction evolution have been documented in literature as shown in Fig. 2.

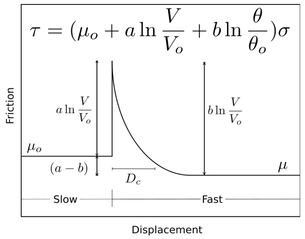

$$\dot{\theta} = 1 - \frac{V\theta}{D_c} \quad \text{(Aging law)}$$

$$\dot{\theta} = -\frac{V\theta}{D_c}\ln\frac{V\theta}{D_c} \quad \text{(Slip law)}$$

Figure 1. Representative plot of friction (μ) as a function of slip displacement during a step change in fault sliding velocity, *V*. Microscale contact strength/area is described by frictional state, θ. Parameters *a* and *b* are constants and D_c is a characteristic distance over which contact lifetimes renew. $\boldsymbol{\tau}$ and σ are shear strength of and normal stresses on the fault. The subscript 'o' signifies an initial condition of the respective parameters

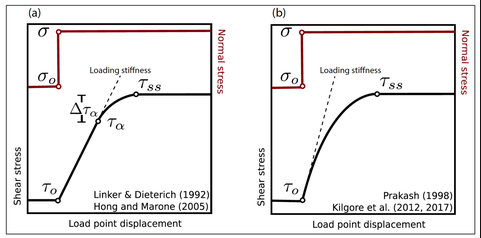

$$\theta = \theta_o\left(\frac{\sigma}{\sigma_o}\right)^{\frac{\alpha}{b}}$$

$$\alpha = \frac{(\tau_{ss}-\tau_\alpha)/\sigma}{\ln\sigma/\sigma_o}$$

Figure 2. On subjecting a fault to a step increase in normal stress from σ_o to σ, (a) a two stage response in shear stress has been documented. Here, the shear stress first increases elastically from $\boldsymbol{\tau}_o$ to $\boldsymbol{\tau}_\alpha$ followed by a non-linear evolution to a steady state value, $\boldsymbol{\tau}_{ss}$. The state evolution formulation for this observation was given by Linker and Dieterich (1992). The parameter 'α' here quantifies the elastic deformation at the contact junctions and (b) A completely non-linear evolution has been suggested by Prakash (1998) and Kilgore et al. (2012, 2017) where either slip or time is necessary for shear stress evolution.

2. Methods

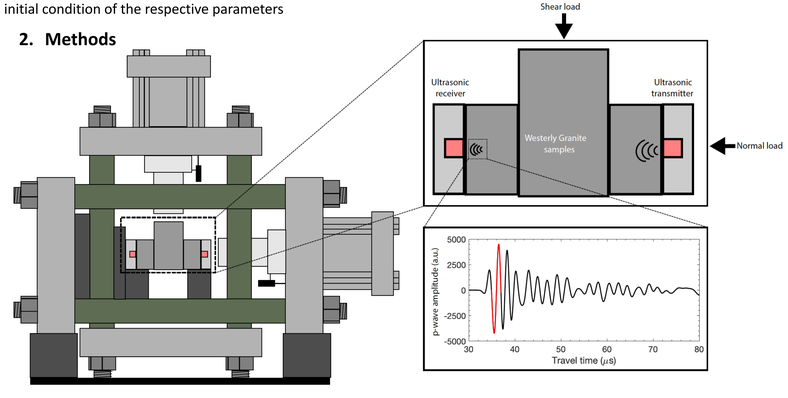

Figure 3. A schematic of the biaxial testing apparatus and Westerly granite blocks used in this study. The setup is instrumented with a load cell and direct current differential transformer (DCDT) transducer in the vertical (shear) and horizontal (normal) stress directions. P-wave polarized piezoelectric transducers on either side of the double-direct shear setup transmit and receive a 500 kHz pulse. A blow-up of a typical wave recorded by the receiver shows the p-wave arrival at ~33 μs. P-wave amplitude is calculated as a peak-to-peak amplitude of the red portion of the waveform.

3. Results

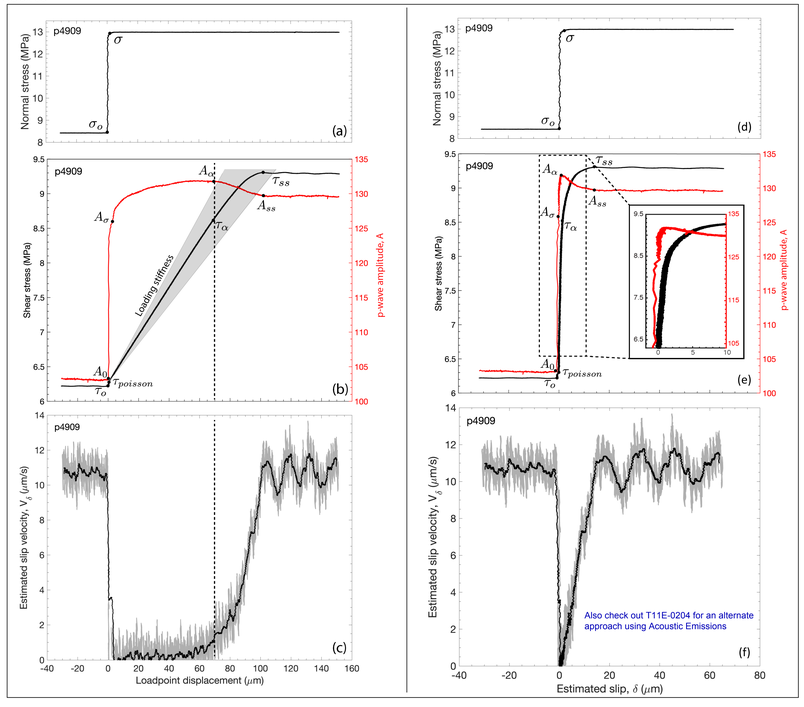

Figure 5. (a) Normal stress step up from 8.4 MPa to 13 MPa (b) The corresponding shear stress increase with load point displacement (black) and acoustic amplitude (red) increase over the same displacement scale. The shaded grey area is the error in calculating load point stiffness (refer to manuscript) and (c) the slip velocity decreases from ~11 μm/s to ~0 μm/s during the normal stress step, as the p-wave amplitude increases. The onset of accelerated fault creep corresponds with a decrease in p-wave amplitude to a steady state value. Panels (d) through (f) express the normal stress, shear stress, amplitude and fault slip velocities as functions of slip.

4. Is ultrasonic amplitude a proxy for real contact area?

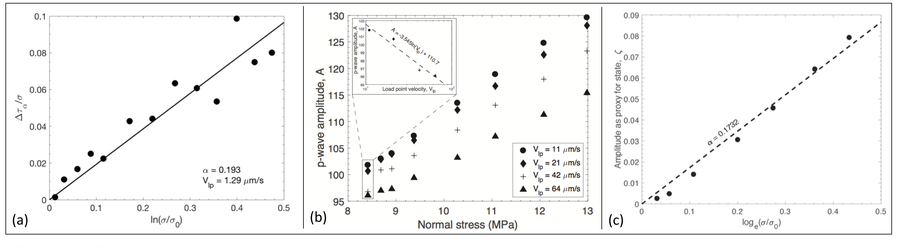

Figure 6. (a) Frictional state evolution term '$\boldsymbol{\alpha}$' constrained from stress data (b) Ultrasonic amplitude varies linearly with normal stress and inverse log-linearly with load-point velocity (inset) (c) Slope of amplitude assumed as proxy for state is equal to '$\boldsymbol{\alpha}$' for normal stress steps

5. Numerical modeling of normal stress steps

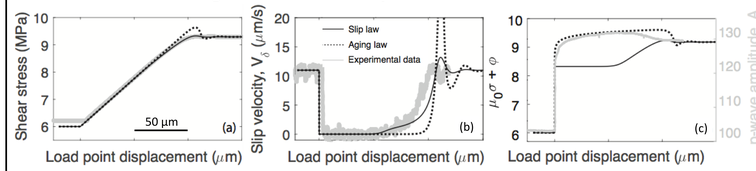

Figure 7. Numerical models of the Slip law match experimental data well for (a) shear stress and (b) slip rate but (c) ultrasonic amplitude is better modeled by Aging law state

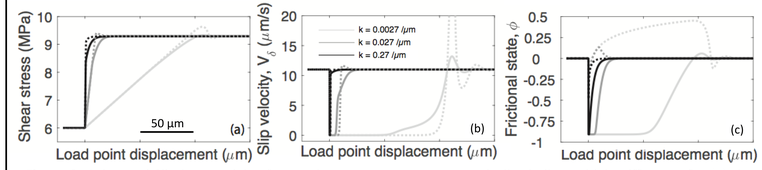

Figure 8. Aging and Slip law models of normal stress steps are asymptotically similar at high stiffnesses for (a) shear stress (b) slip rate and (c) frictional state

6. A microphysical model for contact area variations during normal stress steps

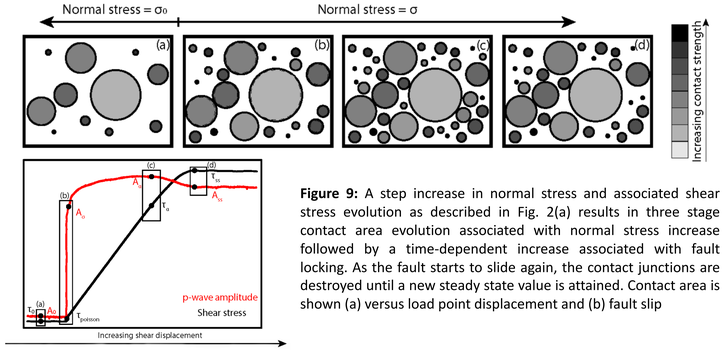

Figure 9: A step increase in normal stress and associated shear stress evolution as described in Fig. 2(a) results in three stage contact area evolution associated with normal stress increase followed by a time-dependent increase associated with fault locking. As the fault starts to slide again, the contact junctions are destroyed until a new steady state value is attained. Contact area is shown (a) versus load point displacement and (b) fault slip

7. Conclusions

- An interplay of apparatus stiffness & large normal stress steps produces an elastic-inelastic shear stress response due to a large slip rate excursion on the fault.
- Large stiffnesses result in a small rate excursion and associated elastic increase which may be unresolved (eg. Prakash, 1998; Kilgore et al., 2012)
- Ultrasonic amplitude could illuminate the evolution of real contact area during shearing.
- The real contact area and steady-state frictional state appear to vary in a complex manner during the normal stress step, and this variation is related to accelerated fault creep.

References

- Hong and Marone (2005). *Geochemistry, Geophysics and Geosystems.* doi: 10.1029/2004GC000821
- Kilgore et al. (2012). *Journal of Applied Mechanics.* doi: 10.1115/1.4005883
- Kilgore et al. (2017). *Journal of Geophysical Research: Solid Earth.* doi: 10.1002/2017JB014049
- Linker and Dieterich. (1992). *Journal of Geophysical Research.* doi: 10.1029/92JB00017
- Prakash. (1998). *Journal of Tribology.* doi: 10.1115/1.2834197

Acknowledgements

This work was supported by a Penn State University Graduate Fellowship to SS, Marie-Curie Fellowship (award 655833) to JR and NSF-1547441 to CJM.